

HEALING OF MANDIBULAR CRITICAL SIZE BONE DEFECTS IN RATS USING PIEZOELECTRIC PLATES: AN IN-VIVO STUDY

Nemat A. Al Ansary^{1*} BDS, Abd El Aziz F. Khalil² PhD, Tamer M. Nassef³ PhD,
Hagar S. Abdel Fattah⁴ PhD, Riham M. Fliefel⁵ PhD

ABSTRACT

INTRODUCTION: "Smart materials" have been introduced as a new concept in bone tissue engineering to improve tissue regeneration and overcome the shortcomings of bone grafts, such as material-related infections, and mechanical failures. Piezoelectric scaffolds are a type of smart material introduced for various biomedical uses such as repair and regeneration of bone tissue.

OBJECTIVES: This study aimed to evaluate the effect of piezoelectric plates in the regeneration of bone and healing of the segmental bone defect in the rat mandible in order to compare their effect with titanium plates.

Materials and Methods: Forty eight rats weighing 275 ± 30 grams were divided into 2 groups: group I; (titanium group), group II; (PVDF poly(vinylidene fluoride) group). Surgical procedures to place the plates were performed in both groups. After first week twenty four of the rats were euthanized and after eight weeks twenty four the rest of rats were euthanized the mandibles were dissected out and prepared for radiographic examination, light microscopic examination and histomorphometry.

RESULTS: Radiographic results showed radio-opacity in the site of the bone defect in both groups. Histological results revealed new bone trabeculae in the both groups, however, bone was more dense and mature in the titanium groups. The histomorphometric analysis also showed substantially higher percentage of new bone per field in the titanium groups.

CONCLUSIONS: piezoelectric plates could enhance bone healing and be used as a mean of achieving good fixation but still the results were inferior to the results of titanium plates.

KEYWORDS: Mandible, Critical-size defects, Bone defects, Rats, Piezoelectric, Fracture.

RUNNING TITLE: Mandibular defects healing in rats using piezoelectric plates.

1 Master student, Department of Oral and Maxillofacial Surgery, Faculty of Dentistry, Alexandria University.

2 Professor of Oral and Maxillofacial Surgery, Department of Oral and Maxillofacial Surgery, Faculty of Dentistry, Alexandria University.

3 Professor of Computer and Software Engineering, Department of Computer and Software Engineering, Misr University for Science and Technology, Cairo.

4 Lecturer of Oral Biology, Department of Oral Biology, Faculty of Dentistry, Alexandria University.

5 Lecturer of Oral and Maxillofacial Surgery, Department of Oral and Maxillofacial Surgery, Faculty of Dentistry, Alexandria University.

*Corresponding author:

E-mail: nematalansary15@gmail.com

INTRODUCTION

Segmental bone defects resulting from bone loss in the maxillofacial region occur due to traumatic injuries, infection, chronic osteomyelitis, non-union or tumor resection. Those defects are difficult and challenging to the maxillofacial surgeons and scientists over the years since there are complex structures including blood vessels, facial skeleton and sensory organs. Besides, Specialists need to manage bacterial contamination in particularly vulnerable sites, such as the nose and oral cavity (1,2). When the segmental defect is too large, bone healing and regeneration is compromised as the

size is more than the intrinsic capability of self-regeneration and as a result bone repair is hindered

and delayed. Accordingly, reconstruction of the maxillofacial segmental defects is mandatory to guarantee the restoration of aesthetic and restore a full rehabilitation of occlusion, articulation and functional capability. Furthermore, reconstruction provides sufficient mechanical strength owing to speech and masticatory processes (2-4).

Large segmental bone defects are improbable. To heal on their own following skeletal stabilization alone. Even though autologous bone grafts are reportedly the gold standard in the repair of segmental

bone defects, there are some issues related to an insufficient supply and morbidity of the donor site. Therefore, the search of new treating methods has emerged strongly in the past few years (5-7).

As an emerging paradigm in bone regeneration, "smart materials" have been developed to improve the tissue healing efficacy to overcome the disadvantages of the traditional materials including infections caused by materials, mechanical failures and unfavourable immunogenic response with the host (6).

Smart materials refer to those materials which can reversibly change one or more of its functional or structural features, according to the installed internal or external stimuli or to the alteration in their surrounding environments (8). The external stimulus varies between physical (temperature, electrical, light or magnetical fields), chemical (pH) or mechanical impulses (stress and strain) (6). Piezoelectric materials have emerged as a class of smart materials with possible medical applications beginning with fabrication of sensors, drug delivery or tissue engineering with major uses in tissue regeneration and repair (9).

Piezoelectricity is the capacity of some solid materials to create an electric field in reaction to implemented mechanical stress. This incident results from the linear electromechanical connection among the mechanical and electrical condition in crystalline substances. Direct piezoelectricity could be observed in tissues such as bone, chondro, dentin, ligament, and keratin (8,10). Piezoelectric materials possess the ability to generate an electrical signal upon exposure to mechanical forces without the need of an external power source for electrical stimulation, which eventually stimulates tissue regrowth where the implant is placed similar to that occurring in natural extracellular matrix (ECM) during the remodeling of bone and cartilage tissue (11).

Various piezoelectric materials have been reported for different biomedical applications including piezopolymers which can be natural substances as collagen or synthetic as poly(vinylidene fluoride) (PVDF), or poly(vinylidene fluoride-trifluoroethylene) (PVDF-TrFE), poly(l-lactic acid) (PLLA) (12).

PVDF is a non-toxic, non-biodegradable, chemically and thermally stable, compatible and flexible piezoelectric polymer (13). Due to those properties, it has been used for a wide range of biomedical implementation, from scaffolds for tissue engineering to implantable self-powered technologies (8). PVDF and its copolymer PVDF-TrFE are of considerable interest in regeneration of bone tissue due to their osteogenic capacity (10) and their piezoelectricity (14). It has greatly facilitated the development of stem cells into osteoblasts from adipose tissue (15).

Despite the fact that the usage of piezoelectric materials for bone regeneration and bone tissue engineering has increased rapidly in recent years, the intricacy of piezoelectric interactions in bone makes the construction of piezoelectric materials extremely difficult. and their suitability for biomedical applications remains unexplored (16).

Thus, the aim of the study was to: a) Fabricate PVDF fracture fixation plates; b) Investigate their stability and mechanical properties; c) Investigate the piezoelectric properties of those plates and d) Evaluate the effect of those plates in healing of a segmental critical size bone defect in the rat mandible.

MATERIALS AND METHODS

Ethical approval and Registration

The current study was examined and approved by the local animal ethics committee's institutional review board, Faculty of Dentistry, Alexandria University (IRB No. 001056-IOrg 0008839-0183-10/2020) under the Guidelines for Animal Experiments of Alexandria University and reported according to the ARRIVE Guidelines (17).

Forty eight 4-month-old Sprague-Dawley rats weighing 275 ± 30 grams were used in this study. The rats were acclimatized for 7 days to the laboratory environment prior to the experiment. The conditions in which the rats were kept was regulated for temperature and humidity, and maintained in plastic cages with availability of food and water ad libitum at 22 ± 2 °C and 12 hour light/dark phases at room temperature. The rats were distributed in cages with four animals per cage.

Sample size calculation and Experimental design

The sample size was calculated using a 5% alpha error and an 80% research power. The mean \pm SD bone volume formed using Titanium plates and PVDF plates after 8 weeks was 5.6 ± 1.06 mm³ (18) and 14.7 ± 4.3 mm³ (19), respectively. Sample size was calculated based in differences between Titanium and PVDF plates using the greatest SD=4.3. The required sample was 5 rats per group which is increased to 6 to compensate for processing issues. Total sample size = Number in each group \times Number of follow up periods \times Number of groups = $6 \times 2 \times 2 = 24$ rats. Software Rosner's technique was used to calculate sample size (20) calculated by G power 3.0.10 (<http://www.gpower.hhu.de/>) (21).

The rats were randomly allocated using an online service (<http://www.randomizer.org/>) (22) into two groups (n=12 per group): (A) The mandibular osteotomy defects were stabilized using the titanium miniplates, (B) The mandibular osteotomy defects were stabilized using the PVDF fixation plates.

Designing of custom-made fixation plate

The custom-made PVDF fracture fixation plates were designed on specialized parametric computer-aided design (CAD) software (Fusion 360, Autodesk, USA). First, the plates were sketched on

2D with the dimensions of 10x3x1 mm. The sketch was extruded to form a plate of 2 mm thickness, then the 3D model was exported from the software as a stereolithographic model (STL). The model was then printed on a masked digital light processing 3D printer (Photon S, Anycubic, China) using a castable resin (Anycubic resin, Anycubic, China). To improve the strength of the PVDF fixation plates, the thickness of the plates (~2 mm) was larger than that of the traditional plates (~1 mm) used in the fixation of the osteotomy defect. Figure 1

Fabrication of PVDF sheets

Poly (vinylidene fluoride) (PVDF, 182702-100G, Mw ~534,000 by GPC) polymer, N,N-Dimethylformamide dimethyl acetal (DMF, 140732) and Acetone (179124-1L) were purchased from Sigma Aldrich (Thalkirchen, Munich, Germany). PVDF sheets were prepared by solvent casting. PVDF sheets at 25% weight was used as the polymer while DMF and acetone (70:30 weight %) were used as mixture solvent without further purification. Briefly, PVDF was homogeneously dissolved in the mixture solvent using a magnetic stirrer. The solution was constantly stirred at 80°C for 3 hours until a clear, homogenous solution was created. The mixed solution was then sonicated at 60°C to remove air bubbles. Dope solution was casted on a 10 cm glass petri dish and set at 4 mm thickness. The produced flat sheets were washed three times with water at 50°C, dried in the open air for 12 hours, and stored in an oven at 40°C for 12 hours.

Hot pressing of PVDF sheets

The solvent casted 4 mm thick PVDF sheet was pressed to a thickness of 2 mm in a 5x5 cm² square shaped die at 140°C and 113kN for 3min using Collin hot-press P300E (Germany). The initial sheets were first cold pressed at 300kN. The temperature was increased from ambient temperature to 140°C. The sheets were then held for 5min under the conditions of 140°C and 300kN. The printed resin models were used as a guide for the cutting of the PVDF fixation plates to the same shape of the plates. Figure 1

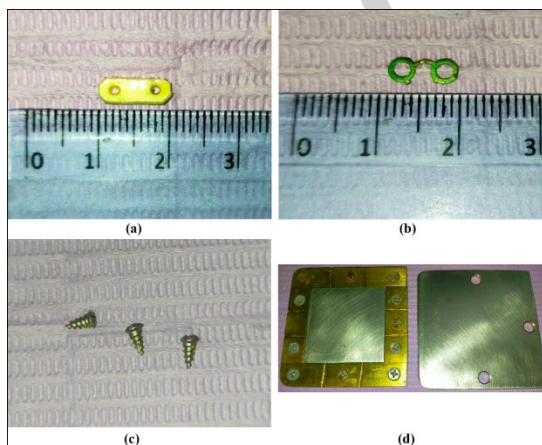


Figure 1: (a) custom made pvdf plate, (b) titanium plate, (c) micro titanium screws, (d) stainless steel

custom made mold for PVDF sheets fabrication.

Three-point bending of the fixation plates

Before implementation in the rat critical-size mandibular defect, the mechanical property of the titanium and PVDF plates was evaluated using a universal material testing machine (ZG-056, MTS Systems Corporation; Eden Prairie, MN) operating in accordance with an ISO standard procedure (YY/T0342-2002). Static three-point bending tests, bending stiffness and the yield load were performed on 3 specimens per group. The inner span measured 20 mm and the outside span measured 40 mm. The mechanical property tests were performed at room temperature at a crosshead speed of 0.05 mm/s.

The osteosynthesis plates were horizontally positioned on two supports. The spread (distance) between the two bottom supports was 6.0 or 10.0 mm. To load the metaphysis, a metallic rod located between the supports and coupled to At 1.0 mm/min, a 50 kgf load cell was released. The loading device and both supports had rounded edges (2.0 mm diameter). During each experiment, the loading device's load and displacement were recorded till breakage. The maximum load at breaking values (N) were determined from the load statistics, and the stiffness (N/mm) was computed as the slope of the curves' first linear uploading section. The needed parameters for the numerical simulations were derived from the test results. Each test was duplicated with three samples to assess the reproducibility of the results, and the mean values and standard deviations (SD) were computed. The mechanical testing was performed according to a previous work (23,24).

Rat Critical size Mandibular defect

The rat mandibular critical size defect was performed according to a previous study (25) the size of the defect performed in this study 5mm. For general anesthesia, Ketamine Hydrochloride (Rotexmedica, Trit- tau, Germany) and Xylazine Hydrochloride (Xyla-ject; Adwia Pharmaceuticals SAE, Cairo, Egypt) diluted to 1:1 was used at a dose of 0.1 ml per 100g body weight in the animal's thigh muscle until deep anesthesia was achieved. A local infiltration of 0.2 ml lidocaine HCl (Amneal Pharmaceuticals) was used to achieve local anaesthesia at a 1:200,000 concentration. The region was antiseptically treated with a 10% betadine solution. (Betadine (The Nile Co. pharmaceuticals)). The animals were placed in a supine position, shaved on the ventral aspect of the jaw and sterilely wrapped. A #15 blade placed on a #3 Bard Barker handle was used to make a 10 mm linear submandibular incision through the skin and periosteum on the right side of the jaw. The inferior border of the jaw was then exposed using electro cautery to divide the pterygomasseteric sling. The buccal and lingual surfaces of the jaw were then accessed by supraperiosteal musculature

elevation. The masseter muscle and periosteum were separated during the dissection, and the flap was retracted with sensitive retractors. Once exposure to the mandible's body was achieved, the osteotomy region was measured and marked. The titanium locking screws of the proper size were used to attach the plate to the bone. The mandibular segmental defect was performed unilaterally with a surgical bur. An osteotomy mandibular defect was created 5mm at the 2nd mandibular molar region at 3,000 RPM with copious sterile saline solution (0.9% sterile sodium chloride) to eliminate bone fragments left inside the defect utilising a syringe. Electrocautery was used to establish hemostasis, and the wound was rinsed to remove bone debris. Each titanium or PVDF plate was repositioned and secured to the created segmental defect. The periosteum reposition to fully cover the defect and the plates and the pterygomasseteric sling was reattached and sutured securely with absorbable Vicryl 5-0 suture (Ghatwary Medical Supply GMS, Alexandria, Egypt). The skin was closed with 4-0 silk intermittent sutures (Ghatwary Medical Supply GMS, Alexandria, Egypt).Figure 2

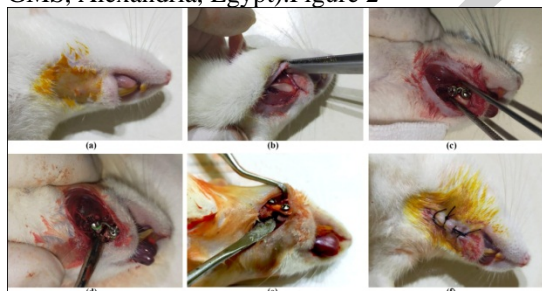


Figure 2: the surgical procedure.

Postoperative Care

Buprenorphine subcutaneous injections were used to analgesize all of the animals. (0.1mg/kg) postoperatively for 72-hours. All animals received antibiotic in the water supply for one week following the surgery as prophylaxis against infections. Animals were fed by a soft diet for the end of the research period. The weights were measured after the first week basis to evaluate nutritional status. All rats were euthanized by administering an overdose of an anesthetic agent at 1 or 8 weeks after the surgery. The mandibles were harvested and fixed in 4% paraformaldehyde (PFA) for further analysis.

Postoperative evaluation

To evaluate the adverse effect of the surgery on the animal diet, the average body weight and dietary intake were measured before the surgery as the baseline and one week after the surgery.

Euthanasia of rats

Six animals of each group were euthanized on week 1 and 8 after surgery with a fatal dose of carbon dioxide, provided at a flow rate of 6 L / minute.

After obvious clinical death, the animals were kept for at least one minute.

Radiographic acquisition

After scarification of the rats, the mandibles were harvested and fixed in ten percent concentration Formaldehyde. The mandibles were then wrapped in tissue paper to remove excess formalin. Radiographs of the specimens was obtained with a plain radiograph apparatus on week 1 and 8 after surgery.

After euthanasation the rats the screws were removed with special screw driver and the plates gripped with tweezers and removed from the defect site All groups' hemimandibles were radiographed with a standard X-ray system. (60 Kvp, 7mA, EZray premium intraoral xray AIRwall) in addition to the digital image capture equipment (Digora, Kavov®, JoinvilleSC, Brazil). The parallel radiographic approach (long cone) utilized an EZ sensor. The hemimandibles were aligned parallel to the radiographic film and the focus-film distance was 6.5 cm with an exposure time of 0.08 seconds.

Radiographic assessment of bone healing

The healing of the bone defects was classified and scored based on the following criteria: 0: No or minimal bone fill (The osteotomy defect stayed radiolucent with the exception of a little amount of new bone formation near the defect borders); 1: limited bone fill (the osteotomy defect was showing regions of radiolucency and radiopacity suggests the emergence of new bone from the borders of the defect without achieving bone continuity.); 2: Complete bone fill (Radiopacity and osseous continuity between the defect borders were visible in the osteotomy defect) (26).

Histological Examination

Overall, the fixed hemi-mandibles were decalcified first. in 5% TCA (Trichloroacetic acid) for one week after that dehydration in a series of ethanol concentration after being washed with water. The biopsies were xylene-cleared, infiltrated, and fixed in paraffin wax. Sections thickness of 4-5µm were sliced by the microtome (KD-2258, Zhejiang Jinhua Kedi Instrumental Equipment, Zhejiang, China). The light microscope (Optika, B-290 series, Ponteranica, Italy) was used to examine all specimens that had been stained with Hematoxylin and Eosin (H&E) to analyze the kind and quality of organic matrix and bone developed. A digital camera (Optika, C-B10, Ponteranica, Italy) was used to take photomicrographs at 100x magnification and The pictures were kept on a computer.

Histomorphometric evaluation of histological samples

Using ImageJ software, computer-assisted histomorphometry analysis was done on the H&E stained sections to contrast the mean Percentage of newly developed bone in the two groups. A single examiner examined the specimens

histomorphometrically blindly. Light microscopy was used to examine sections at a standardized magnification of 100x from the most coronal to the most apical extent. The percentage of bone produced and the percentage of fibrous tissue each field were recorded.

The following formula was used to compute the ratio of new bone to overall area:

$$\text{Percentage of new bone formation} = \frac{\text{New Bone Area}}{\text{Total Area}} \times 100$$

Statistical analysis

The Shapiro Wilk test, box plots, and descriptive statistics were used to determine normality. Variables was presented using Mean and Standard deviation. contrast between the groups were done using Kruskal Wallis after that pairwise comparisons with Bonferroni correction. Intragroup comparisons (across time intervals) were done utilizing Friedman test, then pairwise comparisons with Bonferroni correction. Mechanical properties of plates were compared between groups utilizing Mann Whitney U test. Significance level was set at p<0.05. All of the tests were two-tailed. Data were analyzed using IBM SPSS Statistics for Windows, Version 23.0. Armonk, NY: IBM.

RESULTS

Clinical examination

Forty six out of the 48 rats survived throughout the experiment. Two rats in titanium group died after the surgery.

Rats' body weight and food intake after surgery There was no statistically significant difference in body weight or food consumption. between the titanium and PVDF group. However, the significant difference in both groups was before and at one week after surgery. Details are shown in Table 1.

Table (1) : Body weight and daily food intake of rats

Group	Weight (grams)		Daily food intake amount (DFIA)		p-value
	Before Surgery	1 week after Surgery	Before Surgery	1 week after Surgery	
Titanium	248.7 ± 32.94	235.7 ± 33.10	33.67 ± 2.99	26.25 ± 3.18	<0.001*
PVDF	251.8 ± 28.28	245.4 ± 29.26	34.17 ± 3.80	25.33 ± 3.10	<0.001*

*Statistically significant difference at p value<=0.05

Mechanical Testing of Titanium and PVDF plates

The titanium curve has a steadily increasing linear deflection till reaching a plateau with a maximum average deflection of 1.72 mm, while the PVDF curve is showing only a linear increase in deflection with a higher maximum deflection than that of titanium at 3.16 mm.

Titanium has shown flexural strength of 147.9±2.89 MPa and a strain of 28.72±0.82% with a flexural modulus of 2982.63±156.85 MPa. The high stiffness of the plate has been reflected in the plate’s behavior during testing, where it has shown resistance to bending then permanent deformation without failure and without returning to its original shape.

On the contrary, PVDF had a lower flexural strength of 32.9±2.50 MPa and lower flexural modulus of 86.49±7.40 MPa yet higher strain at 52.67±2.03% compared to titanium.so it takes in consideration when manufacturing and designing of the PVDF plates that the thickness of the plate should not be less than 2mm The higher deflection and lower stiffness were depicted by the ease of bending, and the regaining of the original shape after removal of load during testing as shown in Table 2.

Table (2): Average Score of Bone fill and Comparison of Grey values among the study groups

	Titanium plates (n=6)	PVDF plates (n=6)	
Average Score of Bone fill			
1 st week	0	0	
8 th week	2	2	
Comparison of Grey values among the study groups			p-value
1 st week	24.3±5.6	37.1±1.8	0.153
8 th week	108.2±27.9	65.8±17.0	0.153

*Statistically significant difference at p value<=0.05

The nature and behavior of both materials can also be observed by calculating the toughness. The polymeric semi-crystalline flexible nature of PVDF has led to an increased toughness at 314.00 J/m compared to 186.67 J/m for the stiffer titanium that showed more resistance to bending indicating a better shock absorption effect for the PVDF.

The high stiffness of titanium coupled with the low deflection and low strain contribute to more fixation of the broken fragments with less movement compared to that of the PVDF. The force-deflection curves of both titanium and PVDF were shown in Figure 3,4. Flexural modulus and stiffness are represented by the slope of the initial linear elastic region and the area below the curve representing the toughness. The results of mechanical tests suggested that the plates were qualified for clinical application.

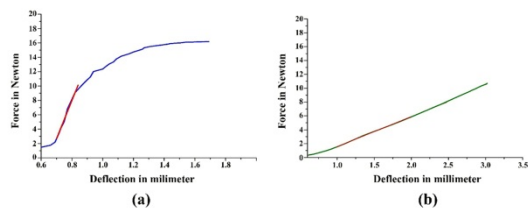


Figure 3: The force-deflection curves of both titanium and PVDF (a): Titanium force-deflection curve. (b): PVDF force-deflection curve.

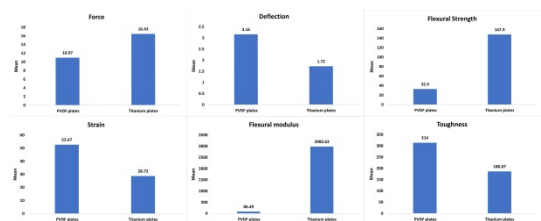


Figure 4: Mechanical Properties of the different fixation plates.

Radiographic findings

In the Titanium group at the 1st week, the radiographic figure 5 showed the radiolucency at the space where the bone defect has been performed while at 8th week, the radiographic figure 5 showed the complete radio opacity at the previous space of the bone defect in comparison to the contralateral side of the same rat.

In the PVDF group at 1st week, the radiographic figure 5 showed the radiolucency at the space of bone defect while at 8th week, the radiographic figure 5 showed the complete radio opacity at the previous space of the bone defect in comparison to the contralateral side of the same rat.

Table 3 show Grey values distribution in different groups and it show that in Titanium plates group it was ranged with a mean value of 24.3 ± 5.6 and it was increased significantly to be at 8th week with a mean value of 108.2 ± 27.9 .and in PVDF plates group it was ranged with a mean value of 37.1 ± 1.80 and it was increased to be at 8th week with a mean value of 65.8 ± 17.0 There were highly statistically significant differences between groups at 1st and 8th weeks

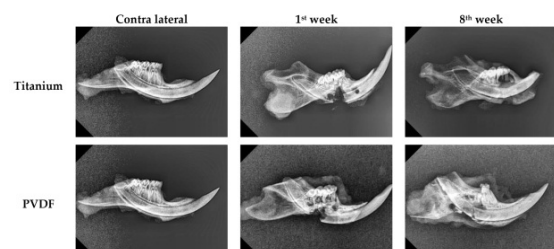


Figure 5: Radiographic findings.

Histological findings

In the Titanium group at the 1st week, the H&E stained sections revealed the bone defect with the hematoma and a condensation of some

inflammatory and mesenchymal cells, some specimen showed thin segments of bone embedded at the center of the defect during the surgical procedure while at 8th week, specimens showed the formation of trabecular of mature spongy bone filling the bone defect. However, areas of cartilage were evident too in addition to bundles of fibrous tissue.

In the PVDF group at 1st week, the bone defect appeared with dense fibrous tissue formation at the center while at 8th week, the results showed the formation of mature trabecular bone surrounding cellular marrow cavities of normal vascularity. However, other sections showed fatty tissue infiltration. Moreover, in some specimens, the absence of bone lining cells was noted. Figure 6

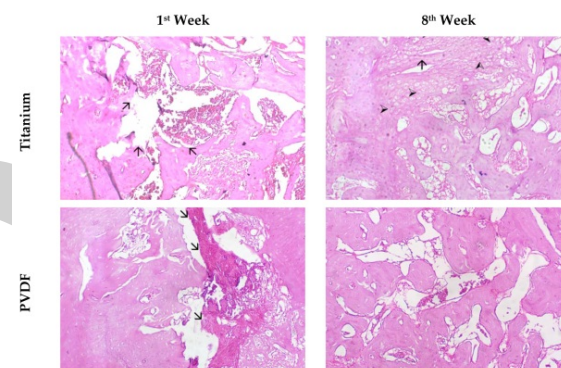


Figure 6: Histological staining of bone using Hematoxylin and Eosin in the different groups. a. Light micrograph (LM) of the titanium group after 1 week showing margins of the bone defect created containing the formed hematoma and condensation of inflammatory cells; b. Light micrograph (LM) of the titanium group after 8 weeks showing the formation of mature bone with the persistence of cartilage (arrow heads) and bundles of fibrous tissue (arrow); c. Light micrograph (LM) of the PVDF group after 1 week showing the bone defect filled with dense fibrous tissue (arrows); d. Light microscope (LM) of the PVDF group after 8 weeks showing the formation of trabecular bone. Note the absence of bone lining cells was noticed. Magnification of 100x.

Biocompatibility assessment of fixation plates

Biocompatibility of titanium plates was evaluated by histological examination that revealed no signs of foreign body reaction, no dense inflammatory cells or fibrous tissue were revealed.

Concerning the pvdf plates, Bundles of fibrous tissue throughout the intervals were revealed and persisted to the end of the 8th week. However, no inflammatory cells were observed. Moreover, the fibrous tissue formed did not prevent the healing and the development of new bone filling the bone defect.

Histomorphometry

The percentage of bone fill measured by histomorphometric analysis revealed significantly higher values in the PVDF group after 1 week in comparison to the titanium group (P=0.0001) However, after 8 weeks The percentage of bone fill was much greater in the titanium group. (P=0.034). Table 3 show bone surface fill percentage distribution in different groups and it show that in Titanium plates group it was with a mean value of 14.34 (3.31) and it was increased significantly to be at 8th week with a mean value of 62.22 (16.07). While in PVDF plates group it was with a mean value of 21.77 (1.07) and it was increased to be at 8th week with a mean value of 38.25 (9.90).

Table (3): Histomorphometry of bone surface fill percentage among the study groups

	Titanium plates (n=6)	PVDF plates (n=6)	P value
1 st week	14.34 (3.31)	21.77 (1.07)	<0.0001
8 th week	62.22 (16.07)	38.25 (9.90)	0.034

*Statistically significant difference at p value≤0.05

DISCUSSION

Our results showed that, in titanium group weight was ranged between 200 – 320 grams with a mean value of 248.7 ± 32.94 grams and it was decreased significantly to be after 1 week after surgery with a mean value of 235.7 ± 33.10 grams while in PVDF group it was ranged between 180 – 307 grams with a mean value of 251.8 ± 28.28 grams and it was decreased significantly to be after 1 week after surgery with a mean value of 245.4 ± 29.26 grams. There were highly differences between the two groups that are statistically significant before and after surgery where P <0.001 and <0.001 respectively. Also, According to daily food intake amount (DFIA) there were highly statistically significant differences between the two groups before surgery where P <0.001 while after 1 week of surgery No statistically significant differences existed between the groups. where P=321.

In similar study had done by Trejo-Iriarte et al (2019) the study was conducted in male and female *Wistar* rats (250–300 g), Animals were fed routinely, and no weight loss was noted during the research; weight was proportional to animal size and age. Morbidity was 0% during the whole research. After 15 days, wound re-epithelialization was noted in roughly 50 percentage of the animals (27).

The current study showed Grey values distribution in different groups and it show that in PVDF plates group it was ranged between 35.6– 39.4 with a mean value of 37.1 ± 1.80 and it was increased to be at 8th week with a mean value of 65.8 ± 17.0 and in Titanium plates group it was ranged between 17.7 – 30.2 with a mean value of 24.3 ± 5.6 and it was increased significantly to be at 8th week with a

mean value of 108.2 ± 27.9. There were highly statistically significant differences between groups at 1st, 4th and 8th weeks where P <0.001, 0.041 and 0.012 respectively.

Langer et al (2018) in report of two cases describes the utilization of a commercially supplied titanium mesh fixed with a novel thermoplastic polymer screw system to repair a calvarial fracture caused by trauma in an adult male Greyhound, as well as a cranioplasty after frontal bone surgical removal in an adult female Cavalier King Charles Spaniel, noted that, The physical examination was within normal ranges during the six-week review. Radiographs and CT scans of the skull indicated a little lifting of the mesh from the frontal bone at its most rostral side (28).

Our results show bone surface fill percentage distribution in different groups and it show that in PVDF plates group it was with a mean value of 21.77 (1.07) and it was increased to be at 8th week with a mean value of 38.25 (9.90) and in Titanium plates group it was with a mean value of 14.34 (3.31) and it was increased significantly to be at 8th week with a mean value of 62.22 (16.07). There were highly statistically significant differences between groups.

According to Yu et al research's (2021) this study involved twenty-four male mice. All of the mice had surgery on the left mandibles. Mandibular deformities of 1.0 mm (n = 8), 1.6 mm (n = 8), and 2.3 mm (n = 8) were created. Micro-computed tomography images and histomorphology were used to investigate bone repair after an 8-week period. Non unions of the mandibular bones were seen 0/8 in the 1.0-mm group, 6/8 in the 1.6-mm group, and 8/8 in the 2.3-mm group. The results of micro-computed tomography revealed that the mineral density of the bone and bone volume to total volume percentage were substantially different among the three groups after 8 weeks. The connective tissue filled the defect area in the nonunion 1.6- and 2.3-mm groups, and no apparent bone growth was observed. Furthermore, quantitative analysis revealed that the percentages in the 1.0-mm, 1.6-mm, and 2.3-mm groups were respectively 91.85 percent and 8.03 percent, 59.84 percent and 20.60 percent, and 15.36 percent and 8.28 percent, indicating statistically significantly poorer healing of defects in the 2.3-mm group (29). Force in PVDF plates group it was ranged between 10.30 - 11.90 with a mean value of 10.97 ± 0.83 while in titanium plates group it was ranged between 16.20 - 16.80 with a mean value of 16.43 ± 0.32. There were statistically significant differences between groups where P=0.049. Deflection in PVDF plates group it was ranged between 3.02 - 3.24 with a mean value of 3.16 ± 0.12 while in titanium plates group it was ranged between 1.69 – 1.78 with a mean value of 1.72 ± 0.05. There were

statistically significant differences between groups where $P=0.049$.

According to Nguyen et al (2013), the mechanical environment has long been recognized to impact the bone healing response. Basically, cortical bone compressive strength ranges between 90 and 230 MPa and breaks at 1.5 percentage compressive longitudinal strain. Trabecular compressive strength spans between 2 and 45 MPa and fails at around 0.7 percent, despite the fact that the stress-strain curve for trabecular bone lacks a well-defined yield point (30).

Flexural Strength in PVDF plates group it was with a mean value of 32.90 ± 2.50 while in titanium plates group it was with a mean value of 147.90 ± 2.89 . There were statistically significant differences between groups where $P=0.049$, Strain in PVDF plates group it was with a mean value of 52.67 ± 2.03 while in titanium plates group it was with a mean value of 28.72 ± 0.82 . Between groups, there were statistically significant differences where $P=0.049$.

Hotchkiss et al (2016) observed that, given the increasing usage of titanium implants hardware in fracture repair surgery and joint prosthesis, Surface modification of Ti has been examined to promote the production of an M2 phenotype. In primary murine BM macrophages, increased M2 polarization was seen by increasing Ti hydrophilicity with oxygen plasma (31).

Flexural modulus in PVDF plates group it was with a mean value of 86.49 ± 7.40 while in titanium plates group it was with a mean value of 2982.63 ± 156.85 . There were statistically significant differences between groups where $P=0.049$ Toughness in PVDF plates group it was with a mean value of 314.00 ± 62.36 while in titanium plates group it was with a mean value of 186.67 ± 5.51 . There were statistically significant differences between groups where $P=0.049$.

In a previous study Ducic et al (2002) reported that, Titanium mesh is biomechanically stable throughout time and can be employed as a scaffolding for soft tissue regeneration over the injured sinus. After proper reconstruction, a complete airtight closure of the sinuses was attained using Soft tissue closure, Ti mesh, and gentamycin-collagen sponge together in the present instances, which remained constant in the long-term monitoring (up to two years) (32).

CONCLUSIONS

Considering the results of the current study, it is concluded that piezoelectric plates can be used as a routine modality for the management of maxillofacial fractures achieving good fixation, and enhanced bone healing.

CONFLICT OF INTEREST

The authors declare that they have no financial or personal conflicts of interest.

FUNDING STATEMENT

There was no special funding provided to the authors for this work.

REFERENCES

1. Fliefel R, Kühnisch J, Ehrenfeld M, Otto S, Gene Therapy for Bone Defects in Oral and Maxillofacial Surgery: A Systematic Review and Meta-Analysis of Animal Studies. *Stem Cells Dev.* 2017;26:215-30.
2. Gaihre B, Uswatta S, Jayasuriya AC. Reconstruction of Craniomaxillofacial Bone Defects Using Tissue-Engineering Strategies with Injectable and Non-Injectable Scaffolds. *J Funct Biomater.* 2017;8:49.
3. Vidal L, Kamplaitner C, Brennan MÁ, Hoornaert A, Layrolle P. Reconstruction of Large Skeletal Defects: Current Clinical Therapeutic Strategies and Future Directions Using 3D Printing. *Front Bioeng Biotechnol.* 2020;8:61.
4. Melville JC, Tran HQ, Bhatti AK, Manon V, Young S, Wong ME. Is Reconstruction of Large Mandibular Defects Using Bioengineering Materials Effective? *J Oral Maxillofac Surg.* 2020;78:661.e1-9.
5. Probst FA, Fliefel R, Burian E, Probst M, Eddicks M, Cornelsen M, et al. Bone regeneration of minipig mandibular defect by adipose derived mesenchymal stem cells seeded tri-calcium phosphate- poly(D,L-lactide-co-glycolide) scaffolds. *Sci Rep.* 2020;10:2062.
6. Zhang K, Wang S, Zhou C, Cheng L, Gao X, Xie X, et al. Advanced smart biomaterials and constructs for hard tissue engineering and regeneration. *Bone Res.* 2018;6:31.
7. Keating JF, Simpson AH, Robinson CM. The management of fractures with bone loss. *J Bone Joint Surg Br.* 2005;87:142-50.
8. Jacob J, More N, Kalia K, Kapusetti G. Piezoelectric smart biomaterials for bone and cartilage tissue engineering. *Inflamm Regen.* 2018;38:2.
9. Tandon B, Blaker JJ, Cartmell SH. Piezoelectric materials as stimulatory biomedical materials and scaffolds for bone repair. *Acta Biomater.* 2018;73:1-20.
10. Kao FC, Chiu PY, Tsai TT, Lin ZH. The application of nanogenerators and piezoelectricity in osteogenesis. *Sci Technol Adv Mater.* 2019;20:1103-17.
11. Przekora A. Current Trends in Fabrication of Biomaterials for Bone and Cartilage Regeneration: Materials Modifications and Biophysical Stimulations. *Int J Mol Sci.* 2019;20:435.
12. Kapat K, Shubhra QTH, Zhou M, Leeuwenburgh S. Piezoelectric Nano-Biomaterials for Biomedicine and Tissue

- Regeneration. *Adv Funct Mater* 2020;30:1909045.
13. Azadian E, Arjmand B, Ardeshiryajimi A, Hosseinzadeh S, Omid M, Khojasteh A. Polyvinyl alcohol modified polyvinylidene fluoride-graphene oxide scaffold promotes osteogenic differentiation potential of human induced pluripotent stem cells. *J Cell Biochem.* 2020;121:3185-96.
 14. Ponnamma D, Parangusan H, Tanvir A, AlMa'adeed MAA. Smart and robust electrospun fabrics of piezoelectric polymer nanocomposite for self-powering electronic textiles. *Mater Des.* 2019;184:108176.
 15. Ribeiro C, Pärssinen J, Sencadas V, Correia V, Miettinen S, Hytönen VP, et al. Dynamic piezoelectric stimulation enhances osteogenic differentiation of human adipose stem cells. *J Biomed Mater Res A.* 2015;103:2172-5.
 16. Mohammadkhah M, Marinkovic D, Zehn M, Checa S. A review on computer modeling of bone piezoelectricity and its application to bone adaptation and regeneration. *Bone.* 2019;127:544-55.
 17. Percie du Sert N, Hurst V, Ahluwalia A, Alam S, Avey MT, Baker M, et al. The ARRIVE guidelines 2019: updated guidelines for reporting animal research. University of Bristol. 2019. Available from: <https://research-information.bris.ac.uk/en/publications/the-arrive-guidelines-2019-updated-guidelines-for-reporting-anima> [Accessed on: Jun, 2022]
 18. Binsalah MA, Ramalingam S, Alkindi M, Nooh N, Al-Hezaimi K. Guided Bone Regeneration of Femoral Segmental Defects using Equine Bone Graft: An In-Vivo Micro-Computed Tomographic Study in Rats. *J Invest Surg.* 2019;32:456-66.
 19. Lopes HB, Santos Tde S, de Oliveira FS, Freitas GP, de Almeida AL, Gimenes R, et al. Poly(vinylidene-trifluoroethylene)/barium titanate composite for in vivo support of bone formation. *J Biomater Appl.* 2014;29:104-12.
 20. Rosner, B. *Fundamentals of Biostatistics*. 8th ed. Boston: Brooks/Cole, Cengage Learning; 2015.
 21. Faul F, Erdfelder E, Buchner A, Lang AG. Statistical power analyses using G*Power 3.1: tests for correlation and regression analyses. *Behav Res Methods.* 2009;41:1149-60.
 22. Research Randomizer. Random Sampling And Random Assignment Made Easy. Research Randomizer. Available from: <https://www.randomizer.org/>.
 23. Zheng B, Deng T, Li M, Huang Z, Zhou H, Li D. Flexural Behavior and Fracture Mechanisms of Short Carbon Fiber Reinforced Polyether-Ether-Ketone Composites at Various Ambient Temperatures. *Polymers (Basel).* 2018;11:18.
 24. Chakladar ND, Harper LT, Parsons AJ. Optimisation of composite bone plates for ulnar transverse fractures. *J Mech Behav Biomed Mater.* 2016;57:334-46.
 25. DeConde AS, Lee MK, Sidell D, Aghaloo T, Lee M, Tetradis S, et al. Defining the critical-sized defect in a rat segmental mandibulectomy model. *JAMA Otolaryngol Head Neck Surg.* 2014;140:58-65.
 26. Kotze MJ, Bütow KW, Kotze HF. A radiological method to evaluate alveolar bone regeneration in the Chacma baboon (*Papio ursinus*). *SADJ.* 2012;67:210-4.
 27. Trejo-Iriarte CG, Serrano-Bello J, Gutiérrez-Escalona R, Mercado-Marques C, García-Honduvilla N, Buján-Varela J, et al. Evaluation of bone regeneration in a critical size cortical bone defect in rat mandible using microCT and histological analysis. *Arch Oral Biol.* 2019;101:165-71.
 28. Langer P, Black C, Egan P, Fitzpatrick N. Treatment of calvarial defects by resorbable and non-resorbable sonic activated polymer pins and mouldable titanium mesh in two dogs: a case report. *BMC Vet Res.* 2018;14:199.
 29. Yu F, Liu L, Xia L, Fang B. Establishment of a C57BL/6 Mandibular Critical-Size Bone Defect Model. *J Craniofac Surg.* 2021;32:2562-5.
 30. Nguyen TL, Gasser A, Nebigil CG. Correction: Nguyen T.L., et al. Role of Prokineticin Receptor-1 in Epicardial Progenitor Cells. *J. Dev. Biol.* 2013, 1, 20-31. *J Dev Biol.* 2020 Dec 11;8(4):32. doi: 10.3390/jdb8040032. Erratum for: *J Dev Biol.* 2013 Jun 18;1(1):20-31. PMID: 33376231; PMCID: PMC7768506.
 31. Hotchkiss KM, Reddy GB, Hyzy SL, Schwartz Z, Boyan BD, Olivares-Navarrete R. Titanium surface characteristics, including topography and wettability, alter macrophage activation. *Acta Biomater.* 2016;31:425-34.
 32. Ducic Y. Titanium mesh and hydroxyapatite cement cranioplasty: a report of 20 cases. *J Oral Maxillofac Surg.* 2002;60:272-6.